Progress in Natural Science: Materials International 2013;23(6):519–523

Chinese Materials Research Society

Progress in Natural Science: Materials International

www.elsevier.com/locate/pnsmi
www.sciencedirect.com

ORIGINAL RESEARCH

Photoresponse and H_2 gas sensing properties of highly oriented Al and Al/Sb doped ZnO thin films

Hannane Benelmadjat[a,*], Boubekeur Boudine[b], Aissa Keffous[c], Noureddine Gabouze[c]

[a]*Laboratoire de Physico-Chimie des Semi-Conducteurs, Département de Physique, Faculté des Sciences Exactes, Université Mentouri-Route Ain Elbey, 25000 Constantine, Algeria*
[b]*Laboratoire de Cristallographie, Département de Physique, Faculté des Sciences Exactes, Université Mentouri-Route Ain Elbey, 25000 Constantine, Algeria*
[c]*Silicon Technology Development Unit, 02 Bd, Frantz Fanon, B.P. 140, Algiers, Algeria*

Received 9 February 2013; accepted 2 July 2013
Available online 23 November 2013

KEYWORDS
Zinc oxide;
Co-doping;
Thin films;
Gas sensing;
Photoresponse

Abstract ZnO:Al and ZnO:Al/Sb thin films have been prepared and investigated. The thin films were deposited on Si substrates by the sol–gel method. The structural, optical and electrical properties of ZnO films have been investigated by spectrophotometry, ellipsometry, X-ray diffraction and current–voltage characterizations. It is found that the films exhibit wurtzite structure with a highly *c*-axis orientation perpendicular to the surface of the substrate, a high reflectivity in the infrared region and a response to illumination. Furthermore, it has been found that Si/(ZnO:Al/Sb)/Al photodiode is promising in photoconduction device while Si/(ZnO:Al)/Al can be used as gas sensor responding to the low H_2 concentrations.

1. Introduction

In last decade, sensitive semiconductor oxides have reached an important place in industrial and technological applications such as in warning systems and space research. Some materials are widely used like silicon and GaN. Among these materials, Al-doped ZnO film is an attractive alternative since it presents good electrical properties with high transparency. Furthermore, zinc oxide is a II–VI semiconductor with a direct wide band gap of 3.3 eV which presents an excellent chemical and thermal stability; it has also the largest exciton binding energy of 60 meV compared with ZnS (20 meV) and GaN (21 meV) [1]. Moreover, ZnO can be prepared at lower temperature than the other two materials. Thanks to these properties, ZnO films find applications in solid-state white-lighting industry, p–n junction UV LED [2], gas sensing [3], blue emitting [4] and photoconductivity [5], as well as in substituting the commonly used transparent conductive oxides (TCO) such as indium tin oxide (ITO) [6]. Several methods have been employed

*Corresponding author. Tel./fax: +213 31 81 88 72.
E-mail address: benelmadjat_hannane@yahoo.fr (H. Benelmadjat).
Peer review under responsibility of Chinese Materials Research Society.

ELSEVIER Production and hosting by Elsevier

1002-0071 © 2013 Chinese Materials Research Society. Production and hosting by Elsevier B.V. All rights reserved.
http://dx.doi.org/10.1016/j.pnsc.2013.11.001

to prepare pure and doped ZnO films such as spray pyrolysis [7], molecular beam epitaxy [8], chemical vapor deposition [9], RF magnetron sputtering [10] and the sol–gel method [11]. The dip coating sol–gel method is easier for elaborating uniform structures with high surface morphology at lower crystallizing temperature and lower cost.

In order to prepare efficient ZnO films, the electrical and structural properties have to be improved, which can be possible by doping of the elements. A variety of dopants have been used like Cu, Al, In, Ga, Sb and N [12,13]. It is expected that introducing some impurities in ZnO results in high electrical conductivity and high optical transparency in the visible range. Al^{+3} is the most used impurity for doping ZnO films, and a lot of studies discussed the importance of this dopant in optical and electrical properties of ZnO films. In order to improve these properties, some authors co-doped ZnO:Al films with other dopants like Sc and Ti [14,15]. But very few works have been aimed on the effect of Sb co-doping in the properties of ZnO:Al films.

In previous work [16], we have studied Sb doped ZnO films. We have found that Sb doping strongly influences the crystallite formation, the optical absorption spectra and the optical band gap, resulting in small sized crystallites and a blue shift of the band gap. The results indicated that ZnO:Sb seems suitable to be used in optoelectronic devices. In this regard, we have introduced few amount of Sb impurities in order to study its influence on the properties of ZnO:Al films. In this work, the structural, optical, light response and gas sensing properties of ZnO:Al and ZnO:Al/Sb films deposited on cleaned Si substrates by the dip coating technique have been studied.

2. Experimental procedure

Zinc acetate dehydrate was used as precursor metal salt; the source of doping was Al $(NO_3)_3 \cdot 9H_2O$ (1% mass) and Sb_2O_3 (0.3% mass). ZnO:Al and ZnO:Al/Sb solutions were prepared by mixing zinc acetate dehydrate and dopants with 2-methoxyethanol, when the solutions turned milky an equimolar amount of monoethanolamine (MEA) was added. The solutions were stirred at 60 °C for 2 h. The final solutions of 0.35 M were clear and homogeneous. The coatings were made 48 h after the solutions were prepared. The post-annealing of the samples was carried out at 350 °C for 10 min in order to evaporate solvents and organic residuals, then the films were annealed at 600 °C for 1 h. The ZnO films were deposited on n-Si substrate with resistivity of 40 Ω cm.

Two structures of Si/(ZnO:Al)/Al and Si/(ZnO:Al/Sb)/Al have been prepared, then photodiode structures of (1.2×1.2 cm^2) were realised with metallic contacts achieved by deposition of 99.99% pure Al on the two sides of the structures.

The crystalline structure of ZnO films was analyzed with X-ray diffraction (XRD) by a Bruker D5000 Advance diffractometer ($\lambda = 1.5402$ Å). Optical properties were carried out using an EL01085306 Varian NIR–UV–vis spectrophotometer 500 Scan and a DRE EL X-02Cellipsometer. The illumination of the photodiodes was done by a Halogen lamp (OSRAM Bellaphot) with a power of 150 W. Gas sensor application was investigated in a stainless steel vacuum chamber (1.43×10^{-3} m^3 vol) kept at room temperature (295 K) and connected by a valve to gas bottles containing hydrogen gas to be used. The current–voltage characteristics of the structures were analyzed for −1.5 V to +1 V bias voltage change against H_2 gas.

3. Results and discussions

XRD studies have been performed in order to determine crystallographic phases. Fig. 1 shows the X-ray diffraction diagrams of ZnO:Al and ZnO:Al/Sb films. ZnO:Al film diagram (curve a) shows two diffraction peaks centered at $2\theta = 34.43°$ and $2\theta = 38.23°$. The peak centered at $2\theta = 34.438°$ belongs to (002) plane of ZnO wurtzite structure, while the other peak centered at $2\theta = 38.234°$ is probably due to Al_2O_3 phase (JCPDS file no. 120539). We remark that the peak related to Al_2O_3 shifts toward small angles when compared with ZnO:Al/Sb and JCPDS file. Whereas, ZnO:Al/Sb film exhibits (curve b) three diffraction peaks centered at $2\theta = 33.29°$, $2\theta = 34.78°$ and $2\theta = 38.49°$. The peak centered at 34.78° related to ZnO wurtzite structure (curve b) exhibits a shift toward large angle when compared to ZnO:Al XRD pattern. While, we think that the two other peaks situated at $2\theta = 33.29°$ and $2\theta = 38.49°$ belong to AlSb (JCPDS file no. 430992) and Al_2O_3 (JCPDS file no. 120539) phases, respectively. The crystallites sizes of the two films were estimated using Scherer's formula [17]

$$D = \frac{0.9\lambda}{B\cos(\theta)} \quad (1)$$

where D is the crystallite diameter, λ is the wavelength, θ is the Bragg angle and B is the full-width at half-maximum (FWMH) of the peak.

The average sizes of crystallites are given in Table 1. The crystallites sizes of ZnO:Al film calculated are found around 29 nm while the crystallites sizes of Al_2O_3 are very small (8.59 nm), which could explain the shift of the diffraction peak toward small angles. In the case of ZnO:Al/Sb film, we remark that

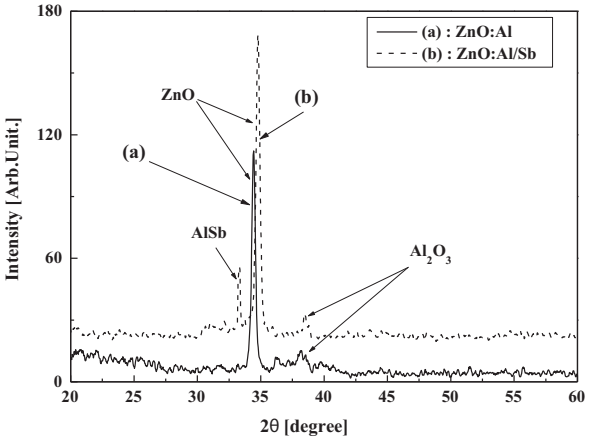

Fig. 1 XRD diagrams of ZnO:Al (curve a) and ZnO:Al/Sb (curve b) films.

Table 1 Crystallites sizes of ZnO: Al and ZnO:Al/Sb films.

	2θ (deg)	FWMH (deg)	Crystallite orientations	Crystallite sizes (nm)
ZnO: Al	34.438	0.286	(002) ZnO	29.054
	38.234	0.198	Al_2O_3	8.591
ZnO:	33.298	0.163	AlSb	50.973
Al/Sb	34.784	0.294	(002) ZnO	28.344
	38.489	0.178	Al_2O_3	47.292

the crystallites sizes of ZnO are similar to those estimated in the case of ZnO:Al, indicating that the use of Sb as dopant does not influence the grain size of the deposited ZnO film. Whereas, the crystallites sizes of the other phases such as AlSb and Al_2O_3, are found of about 50.93 nm and 47.29 nm, respectively. The crystallites sizes values are higher compared with that of ZnO:Al film; it is considered that the presence of Sb may promote the growth of these two phases since Al_2O_3 is known to be formed at about 200 °C [18]. The shift of the ZnO peaks could be due to the difference between Al and Sb ions diameters, which probably induces a compressive strain in the film.

In order to explain the shift of the peak related to ZnO:Al/Sb toward large angles, we have calculated the c parameter of the films using XRD pattern and the following relation:

$$d_{hkl} = \frac{a}{\sqrt{(4/3)(h^2 + k^2 + hk) + l^2(a^2/c^2)}} \quad (2)$$

where h, k, and l are the miller indices, and a and c are the cell parameters.

The lattice parameter c is found to be 5.152 Å for ZnO:Al film and 5.202 Å for ZnO:Al/Sb film, showing that the lattice parameter of the co-doped film is found to be greater than the doped one. For Sb doped ZnO:Al films the increase in the lattice parameter c would be expected when Zn^{++} ions are replaced by Sb^{+3} ions due to mismatch in ionic radii [19]. Another possibility for the increase in the lattice parameters could be due to the formation of electrically inactive Sb_{Zn}–Sb_i pairs described by Wardle et al. [20]. In this regard, we have calculated the strains using the following relations [21]:

$$\sigma = \left[2C_{13} - \frac{(C_{11} + C_{12})C_{33}^{film}}{C_{13}}\right] e_{zz} \quad (3)$$

$$C_{33}^{film} = \frac{0.99 C_{33}^{cristal}}{(1 - e_{zz})^4}$$

and $e_{zz} = (C_0 - C)/C_0$

where C_{ij} are the elastic constants of zincite. C_0 is the strains free lattice parameter (JCPDS file 36-1451).

We find a strain value of −0.382 GPa in the case of ZnO:Al film and −4.979 GPa for ZnO:Al/Sb one. According to these estimations, we can note that the strains are compressive. This result explains why the c parameter of the co-doped film is smaller than the doped one and also the shift of the peak related to ZnO:Al/Sb film toward high angle values. We can conclude that, the introduction of Sb in ZnO:Al lattice causes compressive strains. This is probably due to the great radius of Sb co-dopant (0.245 nm in the case of Sb^{-3} ion).

The reflection spectra of ZnO:Al and ZnO:Al/Sb films measured in the wavelength range of 250–2500 nm are depicted in Fig. 2. It shows that the two films exhibit high reflection in the infrared region. An abrupt decrease of the reflection in the near infrared region is also observed. It is well known that, when off toward the infrared region, the imaginary part of refractive index increases with increasing wavelength, and the variation of the refractive index leads to a sharp increase in reflection of the film.

The effect of Sb co-dopant appears on the reflection spectrum (curve a) as a slight shift towards high wavelength when compared with ZnO:Al spectrum (curve b). In order to explain this shift, several parameters must be known such as the free electrons concentration.

From reflection spectra, free electrons concentration can be calculated in the near infrared region from plasma frequency of the films. The minimum value of reflection corresponds to the minimum frequency and depends on the free electrons concentration by the following relation:

$$\omega_{min} = \left[\frac{Ne^2}{\varepsilon_0(\varepsilon_\infty - 1)m^*}\right]^{1/2} \quad (4)$$

where ω_{min} is the minimum value of reflection, N is the free electrons concentration, ε_0 is the vacuum permittivity, ε_∞ is the dielectric constant of ZnO, m^* is the effective mass of electron and e is the charge of electron.The results of N obtained are given in Table 2. We remark that the free electrons concentration N of (ZnO:Al/Sb) is greater than that of ZnO:Al. This indicates that the presence of Sb ions provides more free electrons. Eq. (4) suggests that ω_{min} increases too, while the wavelength decreases, which means that the reflection spectrum will be shifted towards the visible region when the concentration of the free electrons increases.

We can also calculate the resistivity and the Hall mobility of the films from the following relations:

$$\rho = R_{sq} d \quad (5)$$

$$\rho = \frac{1}{e\mu N} \quad (6)$$

where ρ is the resistivity of the film, R_{sq} is the square resistance of

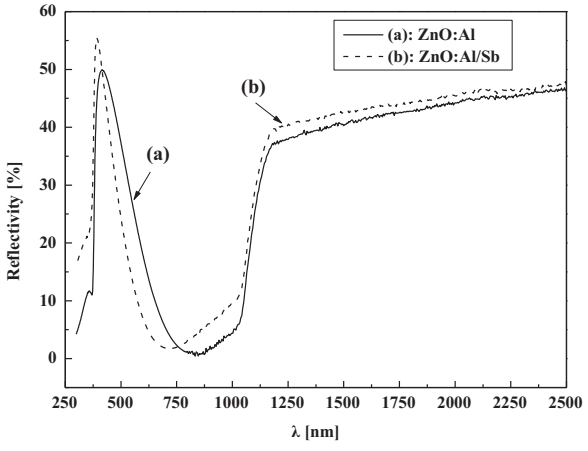

Fig. 2 Reflection spectra of ZnO:Al/Sb (curve a) and ZnO:Al (curve b) films.

Table 2 Free electrons concentrations, resistivity and the Hall mobility of ZnO:Al and ZnO:Al/Sb films.

	λ_{min} (nm)	W_{min} (cm^{-1}) × 10^{12}	N (cm^{-3}) × 10^{19}	d (nm)	R_{sq} (Ω) × 10^3	ρ (Ω cm)	μ (cm^2/V s)
ZnO:Al	833.52	3.59	4.99	80.15	39.36	0.315	0.39
ZnO:Al/Sb	718.06	4.18	6.73	84.00	22.41	0.188	0.79

the film, d is the thickness of the film estimated by ellipsometry measurements (Table 2), e is the charge of electron, μ is the Hall mobility of the film and N is the free electrons concentration.

The thickness of ZnO:Al and ZnO:Al/Sb films measured by ellipsometry measurement (shown in Table 2) has been found to be 80.15 nm and 84 nm, values slightly similar.

From Table 2, we note values of electrical resistivity of 0.188 Ω cm and 0.315 Ω cm for ZnO:Al/Sb and ZnO:Al, respectively. It clearly appears that the resistivity of the co-doped film is smaller than the Al-doped one. Moreover, the mobility of (ZnO:Al):Sb film is found to be greater than that of ZnO:Al film.

When Al is introduced in the ZnO matrix, it occupies the sites of Zn atoms. The replacement of Zn^{+2} ions with Al^{+3} leads to n-type doping, which results in the increase in carrier concentration. However, when ZnO doped Al is co-doped with a certain concentration of Sb we note the increase of carrier concentration and the decrease of resistivity of the films. It is considered that, small amount of Sb^{+3} ions provides more free electrons and results in the decrease in the resistivity of the films.

4. Applications

4.1. Photodiode application

The photodiode structure realized is shown in Fig. 3. The current–voltage (I–V) characteristics of the structures in the dark and under illumination are depicted in Fig. 4. A rectifying behavior can be observed in the I–V curves in the dark of Si/(ZnO:Al)/Al (curve a) and Si/(ZnO:Al/Sb)/Al (curve b) diodes, which suggest a Schottky diode. We remark that, the direct bias current depends strongly on the presence of illumination. Curves aL (light) and bL (light) of Fig. 4 indicate the current obtained under illumination of the two studied structures. It is found that for both structures the photogenerated current (I_{ph}) increases with increasing bias voltage. Moreover, we observed also, that the photocurrent ($I_{ph}=I_{light}-I_{dark}$), where I_{light} and I_{dark} are the currents obtained in light and dark respectively, is more important in the case of ZnO:Al/Sb film than that of ZnO:Al. This result clearly indicates that the introduction of Sb in the ZnO:Al film improves the electrical (photo) response of the structure and increases the photoelectrical performances of the structure. The results are in good agreement with those reported in Table 2.

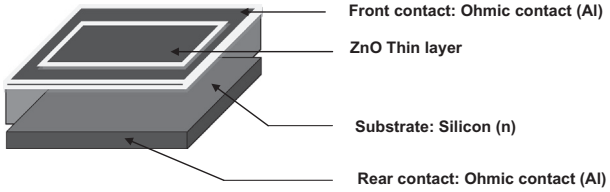

Fig. 3 Schematic diagram of the photodiode and the gas sensor structure.

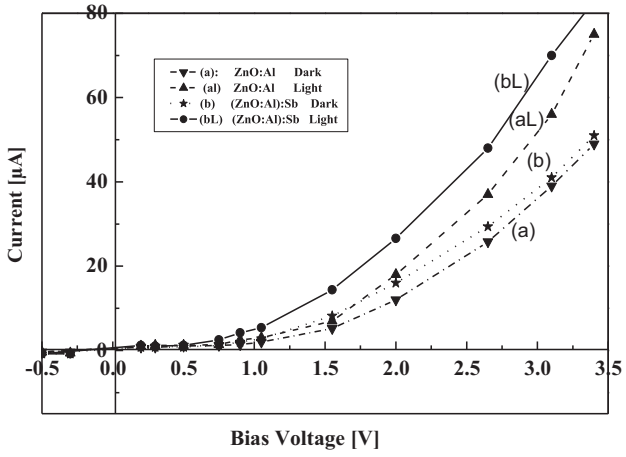

Fig. 4 Dark and light I–V characteristics of ZnO:Al/Si and ZnO:Al/Sb/Si ZnO:Al/Sb with illumination (curve aL), without illumination (curve a), ZnO:Al with illumination (curve bL), and without illumination (curve b).

4.2. Gas sensor application

The Si/(ZnO:Al)/Al and Si/(ZnO:Al/Sb)/Al structures (Fig. 3) have been used to investigate their gas sensing properties. Fig. 5 shows the I–V curves of the ZnO:Al based sensor under air and against different H_2 gas concentrations. One can observe that, for positive bias voltage the variation $|\Delta I|=|I-I_{air}|$, where I_{air} and I corre-

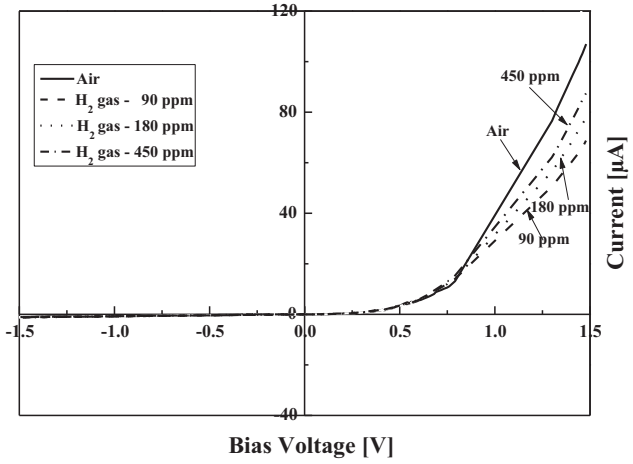

Fig. 5 I–V characteristics of Si/(ZnO:Al)/Al on air and against different H_2 gas concentrations.

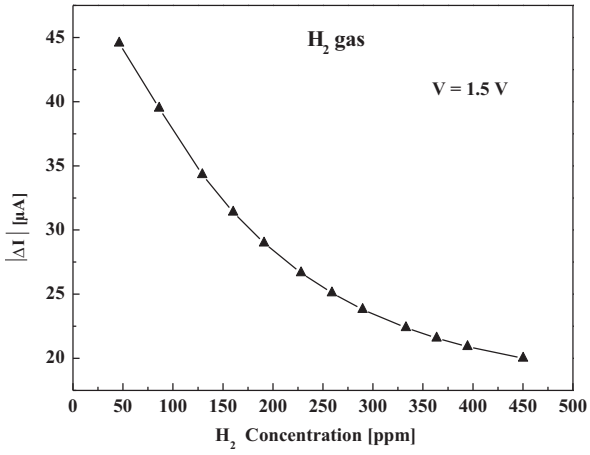

Fig. 6 Variation of current of Si/(ZnO:Al)/Al structure with H_2 gas concentration at bias potential of +1.5 V.

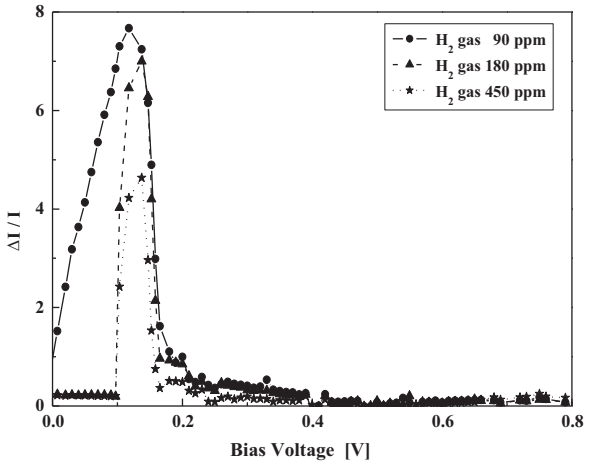

Fig. 7 Variation of sensitivity of Si/(ZnO:Al)/Al structure as a function of bias voltage for several H_2 gas concentration.

spond to currents acquired before and after contact with H_2 gas, is negative for H_2 gas, indicating that, hydrogen behaves as a reducing gas on the Si/(ZnO:Al)/Al structure. In addition, it is shown in Fig. 6 that at a bias voltage of +1.5 V the current variation $|\Delta I|$ value is first maximum for a gas concentration of 50 ppm and then decreases with higher concentration of H_2. Whereas, we noted that the Si/(ZnO:Al/Sb)/Al structures are not influenced by the presence of H_2 gas and no variation in the current has been noted. Moreover, the structure was also shown to be insensitive to cigarette smoke which contains several gases (oxidant and reducing gases). At first glance, it appears that Sb as co-dopant plays an important role in the phenomenon of H_2 adsorption. This striking feature is currently under study in order to determine its (Sb) contribution in the detection of H_2 gas. Finally, the sensitivity ($S=|\Delta I|/I$) of the Si/(ZnO:Al)/Al structure for three concentrations of hydrogen gas (90, 180 and 450 ppm) as a function of bias voltage has been measured (Fig. 7). It is shown that, the sensitivity increases when increasing bias voltage reaches a maximum at 0.12 V, corresponding to the maximum sensitivity, then decreases. In addition it is noted that the sensitivity decreases with increasing H_2 gas concentration. This result clearly indicates that the high sensitivity of the structure is observed for low concentration of H_2 gas.

5. Conclusion

In this paper, ZnO:Al and ZnO:Al/Sb films were prepared with the sol–gel method and deposited by the dip coating technique on Si substrates. Structural characterization by XRD shows a highly oriented ZnO wurtzite structure with the formation of Al_2O_3 phase and AlSb in the case of Sb co-doping. Carrier concentration, electrical resistivity and light response of the films are found to be improved by Sb introduction. So, the Si/(ZnO:Al/Sb)/Al structure is very promising in photoconduction devices. The results of gas sensing with several H_2 gas concentrations presented in this work show that, only the developed Si/(ZnO:Al)/Al structure can be used as gas sensor and responds to H_2 gas with high sensitivity to low H_2 concentration. Finally, the results prove that both ZnO:Al and ZnO:Al/Sb films can be used in photovoltaic cells and optoelectronic devices.

References

[1] B. Lin, Z. Fu, Y. Jia, Appl. Phys. Lett. 79 (2001) 943.
[2] D.C. Kim, W.S. Han, B.H. Kong, H.K. Cho, C.H. Hong, Phys. B: Condens. Matter 401–402 (2007) 386–390.
[3] K. Arshak, I. Gaidan, E.G. Moore, C. Cunniffe, Superlattices Microstruct. 42 (2007) 348–356.
[4] J. Zhang, H. Feng, W. Hao, T. Wang, J. Sol–Gel Sci. Technol. 39 (2006) 37–39.
[5] Z. Xu, H. Deng, J. Xie, Y. Li, Y. Li, J. Sol–Gel Sci. Technol. 36 (2005) 223–226.
[6] T. Minami, Thin Solid Films 516 (2008) 5822–5828.
[7] J. Benny, K.G. Gopchandran, P.K. Manoj, P. Koshy, V.K. Vaidyan, Bull. Mater. Sci. 22 (1999) 921–926.
[8] Y. Feng, Y. Zhou, Y. Liu, G. Zhang, X. Zhang, J. Lumin. 120 (2006) 233–236.
[9] H. Funakubo, N. Mizutani, M. Yonetsu, A. Saiki, K. Shinozaki, J. Electroceram. 4 (1999) 25–32.
[10] W. Lail, C.T. Lee, Mater. Chem. Phys. 110 (2008) 393–396.
[11] H. Benelmadjat, B. Boudine, O. Halimi, M. Sebais, Opt. Laser Technol. 41 (2009) 630–633.
[12] T. Ratana, P. Amornpitoksuk, T. Ratana, S. Suwanboon, J. Alloys Compd. 470 (2009) 408–412.
[13] S. Ilican, Y. Caglar, M. Caglar, F. Yakuphanoglu, J. Cui, Physica E 41 (2008) 96–100.
[14] J. Chen, D. Chen, J. He, S. Zhang, Z. Chen, Appl. Surf. Sci. 255 (2009) 9413–9419.
[15] M. Jiang, X. Liu, Appl. Surf. Sci. 255 (2008) 3175–3178.
[16] H. Benelmadjat, N. Touka, B. Harieche, B. Boudine, O. Halimi, M. Sebais, Opt. Mater. 32 (2010) 764–767.
[17] A. Davydov, A. Glebkin, Izv. Akad. Nauk. SSSR Neorg. Mater. 8 (1972) 883–899.
[18] S. Bernik, N. Daneu, J. Eur. Ceram. Soc. 27 (2007) 3161–3170.
[19] O. Lupan, L. Chow, L.K. Ono, B.R. Cuenya, G. Chai, H. Khallaf, S. Park, A. Shultz, J. Phys. Chem. C (2010) 12401–12408.
[20] M.G. Wardle, J.P. Goss, P.R. Briddon, Phys. Rev. B 71 (2005) 155205.
[21] K.T. Ramakrisha Reddy, T.B.S. Reddy, I. Forbes, R.W. Miles, Surf. Coat. Technol. 151–152 (2002) 110–113.